MINERALOGY OF ANTARCTIC AUBRITES, YAMATO-793592 AND ALLAN HILLS-78113: COMPARISON WITH NON-ANTARCTIC AUBRITES AND E-CHONDRITES

Makoto Kimura[1], Yang-Ting Lin[2], Yukio Ikeda[1],
Ahmed El Goresy[3], Keizo Yanai[4]
and Hideyasu Kojima[4]

[1] *Department of Earth Sciences, Faculty of Science, Ibaraki University,*
1–1, Bunkyo 2-chome, Mito 310
[2] *Institute of Geochemistry, Academica Sinica, Wushan,*
Guanzhou 510640, China
[3] *Max-Planck Institut für Kernphysik, Postfach 103 980,*
D-6900 Heidelberg, Germany
[4] *National Institute of Polar Research, 9–10, Kaga 1-chome,*
Itabashi-ku, Tokyo 173

Abstract: Two Antarctic aubrites, Yamato (Y)-793592 and Allan Hills (ALH)-78113, were mineralogically studied, for comparison with minerals in non-Antarctic aubrites and enstatite chondrites. The Antarctic aubrites are breccias consisting of coarse-grained enstatite fragments and fine-grained matrix. ALH-78113 has 200–300 μm dark clasts that are fine-grained aggregates of silicate and opaque minerals. FeO-rich pyroxene (up to Fs_{21}) occurs in the dark clasts. One dark clast has K-feldspar. These dark clasts seem to be exotic inclusions with distinct mineralogy. Daubreelite in the two Antarctic and non-Antarctic aubrites is lower in Zn than those in EH3-5 chondrites. This reflects the depletion of volatile elements in aubrites. Hydrated Na-Cr-sulfides were also found. Djerfisherite is a common accessory mineral in aubrites. It is characterized by low contents of Cu and Na, and high content of Ni, in comparison to djerfisherite in EH3-5 chondrites. Y-793592 has many roedderite grains. The occurrences of roedderite, Na-Cr-sulfides and djerfisherite in aubrites suggest that Al_2O_3 relative to alkali elements may have been fractionated during nebular or magmatic process.

1. Introduction

Aubrites are meteorites that consist mainly of nearly pure enstatite with various accessory minerals including distinct sulfides. Although aubrites are of igneous origin (Watters and Prinz, 1979; Wolf *et al.*, 1983), they have oxygen isotopic compositions (Mayeda and Clayton, 1980) and mineral assemblage similar to those of enstatite chondrites. All these enstatite meteorites formed under highly reducing conditions. The origin of aubrites is controversial. Watters and Prinz (1979) suggested that aubrites were derived from a magma of EL6 composition, although plagioclase was fractionated in aubrites. Keil (1969) reported higher Ti contents of troilite in aubrites than those in enstatite chondrites. Keil (1969) and Brett and Keil (1986) suggested that aubrites

186

were not derived from known enstatite chondrites on the same parent body, because there is no mechanism for high concentration of Ti-rich troilite in aubrites during magmatism, and no enstatite chondritic clasts in aubrites are encountered. In addition, KEIL (1989) pointed out that abundant diopside in aubrites cannot be derived from an enstatite chondritic material by magmatism.

We have carried out a detailed mineralogical study of two Antarctic aubrites, Y-793592 and ALH-78113, using a scanning electron microscope (SEM). Y-793592 is the first aubrite in the Yamato meteorite collections and was described by YANAI and KOJIMA (1991) and YANAI (1992). ALH-78113 was first described by WATTERS et al. (1980). For comparison, we also analyzed some accessory minerals in non-Antarctic aubrites, Aubres, Bustee, Cumberland Falls (achondritic part), Khor Temiki and Peña Blanca Spring, from the Max-Planck-Institut für Kernphysik collection. On the basis of these data, we discuss the mineralogical features of aubrites in comparison to EH and EL chondrites.

2. Experimental Methods

Quantitative analyses of minerals were performed with JEOL 733 and SEMQ type wave length-dispersive electron-probe microanalyzers (EPMA). The accelerating voltage and beam current were 15 kV and 3 to 10 nA, respectively. The Bence-Albee correction method was used for the analysis of silicates, and the ZAF method was used for sulfides and metals. A special deconvolution program was applied to correct for X-ray overlaps of K_β on K_α lines of some successive elements such as Cr-Mn, Fe-Co and Ni-Cu.

3. Petrography and Mineralogy

3.1. Y-793592

Y-793592 is a monomict breccia consisting of coarse-grained enstatite fragments, up to 5 mm, with fine-grained matrix. Such a structure is typical of common aubrites (WATTERS and PRINZ, 1979). The matrix consists of enstatite with diopside, olivine, plagioclase, a silica mineral, glass and opaque minerals (Table 1). Phases in the matrix are usually small in size (below 200 μm). Although the abundance of opaque minerals in aubrites is fairly small (WATTERS and PRINZ, 1979), opaque minerals occur predominantly in the matrix as isolated grains or aggregates of a few minerals. Y-793592 displays shock metamorphic features; mechanical twinning of enstatite and troilite, and wavy extinction of olivine.

Enstatite in Y-793592 is almost homogeneous in composition, $En_{97.8-99.8}$ $Fs_{0.0-0.2}Wo_{0.2-2.2}$ (Table 2). Diopside is $En_{51.8-56.6}Fs_{0.0-0.1}Wo_{43.3-48.2}$ in composition (Fig. 1a). Olivine is pure forsterite. Most of plagioclase is sodic ($Ab_{93.3-97.4}$ $An_{0.0-4.1}Or_{2.2-4.8}$), but a few CaO-rich plagioclase fragments ($Ab_{76.0-89.9}An_{7.4-23.1}$ $Or_{0.9-3.7}$) occur (Fig. 3). The compositions of plagioclases are in the range of non-Antarctic aubrites ($Ab_{75-95}An_{2-24}Or_{1-5}$ after WATTERS and PRINZ, 1979). Glass fills the interstices between mineral fragments, and is usually rich in SiO_2 (60.2–78.2 wt%), Al_2O_3 (2.0–20.8%) and Na_2O (0.1–10.9%). Most of the glass are enriched in normative feldspar. A silica mineral grain occurs in the matrix and appears

Table 1.   Constituent phases in Y-793592 and ALH-78113.

Meteorite	Y-793592		ALH-78113			EH3–5	EL6
Component	Coarse pyroxene fragment	Matrix	Coarse pyroxene fragment	Matrix	Dark clast		
Enstatite	+	+	+	+	+	+	+
Diopside		+	+	+	+	+	
Olivine		+		+	+	+	
Plagioclase		+		+	+	+	+
K-feldspar					+		
Silica mineral		+		+		+	+
Roedderite		+				+	
Glass		+		+	+	+	
Fe–Ni metal	+	+	+	+	+	+	+
Schreibersite		+		+	+	+	+
Troilite	+	+	+	+	+	+	+
Alabandite		+		+	+		+
Niningerite						+	
Oldhamite						+	+
Sphalerite						+	+
Daubreelite		+		+	+	+	+
Djerfisherite		+		+		+	
Na-Cr-sulfide		+				+	

Minerals in EH3–5 and EL6 after Keil (1968), El Goresy *et al.* (1988), and Kimura and El Goresy (1988). Only representative minerals in EH3–5 and EL6 are listed here.

to be quartz (Fig. 1a). Y-793592 has many roedderite grains, 20-50 μm in size, in the matrix, which usually show irregular to rectangular shapes (Fig. 1a). Roedderite has 0.3–0.9 wt% Al_2O_3, <0.1% FeO, 3.1–3.4% Na_2O and 4.2–4.9% K_2O. Roedderite in aubrite was found only from LEW87294 (Ntaflos and Koeberl, 1992), although its composition was not reported.

Kamacite and taenite occur rarely in enstatite fragments and the matrix. Kamacite and taenite have 2.4–5.3 and 34.5 wt% Ni, respectively (Table 3). Schreibersite (16.7 wt% Ni) also rarely occurs in the matrix. Troilite has 0.1–8.5 wt% Ti and 0.2–0.7% Cr (Table 4). The high Ti content of troilite is typical of aubrites (Fig. 4). Daubreelite often occurs as isolated grains that contain 0.6–2.0 wt% Mn and 0.0–0.3% Zn. Alabandite and djerfisherite have suffered severe terrestrial weathering. Djerfisherite has 0.3 wt% Na, 7.9% K, 1.3% Ni and 0.2% Cu.

Caswellsilverite was not found in the aubrites studied here. Instead, Y-793592 has a few grains of another Na-Cr-sulfide, 10–20 μm in size (Fig. 1b). They are often in association with troilite, and occur in the matrix. These grains always consist of bright and dark areas under back-scattered electron image. Such a structure is typical of intergrowth of minerals A and B which were reported in EH chondrites by El Goresy *et al.* (1988). Bright (mineral A) and dark (mineral B) areas of Na-Cr-sulfides in Y-793592

Table 2. Representative chemical compositions of silicate phases (wt%).

Phase	Meteorite	Occ.	SiO_2	TiO_2	Al_2O_3	Cr_2O_3	FeO	MnO	MgO	CaO	Na_2O	K_2O	Total	Fo	Or/En	Ab/Fs	An/Wo
Feldspar	Y-793592	2	68.2	0.00	19.7	0.00	0.03	0.00	0.00	0.40	11.4	0.69	100.4		3.8	94.3	1.9
	Y-793592	2	62.5	0.00	23.2	0.00	0.05	0.00	0.00	5.19	9.5	0.18	100.6		0.9	76.0	23.1
	ALH-78113	2	57.6	0.00	25.7	0.00	0.00	0.00	0.07	8.24	7.4	0.09	99.1		0.5	61.6	37.9
	ALH-78113	2	68.6	0.00	19.2	0.00	0.00	0.00	0.00	0.15	11.5	0.31	99.9		1.7	97.6	0.7
	ALH-78113	3	64.4	0.00	17.7	0.00	0.08	0.00	0.31	0.02	1.3	15.2	98.9		88.4	11.5	0.1
Glass	Y-793592	2	70.8	0.00	17.0	0.00	0.05	0.11	2.97	0.00	8.93	0.61	100.5				
	ALH-78113	2	74.2	0.00	14.5	0.00	0.00	0.00	0.79	0.08	7.62	1.24	98.4				
	ALH-78113	3	61.8	0.04	12.2	0.22	1.61	0.00	7.59	9.07	6.70	0.22	99.4				
Olivine	Y-793592	2	43.1	0.00	0.00	0.00	0.00	0.03	56.6	0.02	0.00	0.01	99.8	100.0			
	ALH-78113	2	42.6	0.00	0.00	0.00	0.00	0.03	57.6	0.07	0.00	0.00	100.2	100.0			
	ALH-78113	3	42.6	0.03	0.08	0.00	1.22	0.09	53.9	0.06	0.02	0.00	98.0	98.7			
Diopside	Y-793592	2	55.2	0.00	0.35	0.00	0.00	0.00	20.1	23.8	0.41	0.00	99.9		54.2	0.0	45.8
	ALH-78113	2	55.7	0.06	0.55	0.00	0.00	0.03	20.4	23.4	0.28	0.00	100.4		54.8	0.0	45.2
	ALH-78113	3	54.4	0.59	0.12	0.13	1.17	0.33	19.2	22.8	0.40	0.02	99.1		52.9	1.8	45.3
Enstatite	Y-793592	1	59.5	0.00	0.05	0.00	0.00	0.00	39.5	0.26	0.00	0.00	99.3		99.5	0.0	0.5
	Y-793592	2	59.8	0.00	0.05	0.00	0.06	0.00	39.5	0.32	0.00	0.00	99.7		99.3	0.1	0.6
	ALH-78113	1	60.1	0.00	0.00	0.00	0.00	0.00	40.2	0.35	0.00	0.00	100.6		99.4	0.0	0.6
	ALH-78113	2	59.7	0.00	0.01	0.00	0.20	0.00	39.3	0.41	0.00	0.00	99.6		98.9	0.3	0.8
	ALH-78113	2-i	55.7	0.00	0.00	0.00	12.6	0.43	29.9	0.18	0.00	0.00	98.8		80.6	19.1	0.4
	ALH-78113	3	56.9	0.15	0.25	0.10	12.4	0.35	29.7	0.35	0.00	0.00	100.2		80.5	18.8	0.7
Roedderite	Y-793592	2	71.5	0.00	0.84	0.00	0.00	0.00	19.7	0.00	3.17	4.51	99.7				
Silica mineral	Y-793592	2	97.9	0.00	1.63	0.00	0.00	0.00	0.00	0.00	0.76	0.02	100.3				
	ALH-78113	2	96.3	0.00	1.74	0.00	0.00	0.00	0.03	0.08	0.79	0.07	99.0				

Occurrence 1: coarse-grained enstatite fragment, 2: matrix, 3: dark clast, 2-i: isolated FeO-rich pyroxene in matrix.
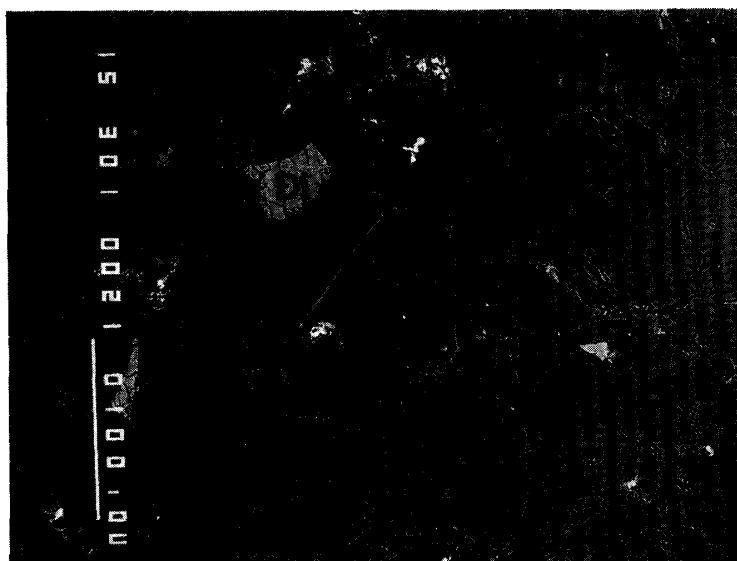
Fig. 1a. Back-scattered electron (BSE) image of diopside (Di), roedderite (Ro) and a silica mineral (Si) in the matrix of Y-793592. The matrix mainly consists of enstatite fragments. White scale bar of 100 μm.
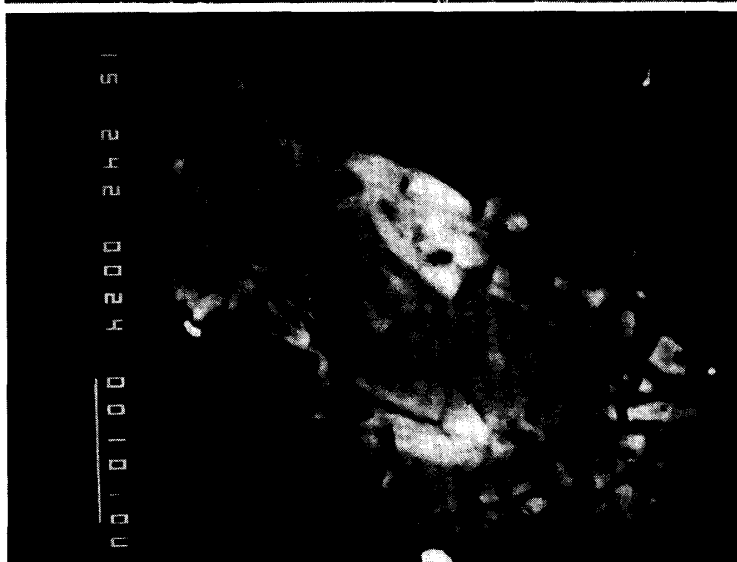

Fig. 1b. A Na-Cr-sulfide grain in Y-793592, consisting of bright (mineral A) and dark (B) areas. BSE image. White scale bar of 10 μm.

Table 3. Representative chemical compositions of metals (wt%).

Mineral	Meteorite	Si	P	Fe	Co	Ni	Total
Kamacite	Y-793592	0.13	0.05	92.9	0.30	4.72	98.7
	ALH-78113	0.11	0.00	94.4	0.39	5.34	100.3
Taenite	Y-793592	0.17	0.04	63.3	0.61	34.5	98.6
	ALH-78113	0.08	0.00	45.6	0.13	51.4	97.3
Schreibersite	Y-793592	0.24	15.4	66.8	0.24	16.7	99.5
	ALH-78113	0.03	15.4	55.5	0.17	27.7	98.8
	ALH-78113	0.05	14.9	26.1	0.10	58.8	99.9

Table 4. Representative chemical compositions of sulfides (wt%).

Mineral	Meteorite	Na	Mg	S	Cl	K	Ca	Ti	Cr	Mn	Fe	Co	Ni	Cu	Zn	Zr	Ag	Total
Alabandite	ALH-78113	—	0.57	36.1	—	—	0.17	—	0.10	52.4	10.6	—	—	—	—	—	—	99.8
	Peña Blanca Spring	—	0.55	36.5	—	—	—	—	0.10	52.3	10.7	—	—	—	—	—	0.00	100.2
	Peña Blanca Spring*	—	0.77	32.9	—	—	—	—	—	47.8	8.75	—	—	—	—	—	10.4	100.6
Daubreelite	Y-793592	—	—	43.9	—	—	—	0.09	35.1	1.69	16.1	—	—	—	0.30	—	—	97.2
	ALH-78113	—	—	43.2	—	—	—	0.05	35.8	1.19	17.7	—	—	—	0.21	—	—	98.2
	Bustee	—	—	44.5	—	—	0.10	0.35	35.9	1.36	17.5	—	—	0.39	0.05	—	—	100.2
	Khor Temiki	—	—	44.8	—	—	0.00	0.09	36.8	0.15	17.1	—	—	0.14	0.13	—	—	99.3
Djerfisherite	ALH-78113	0.50	—	32.2	1.45	8.14	—	—	—	—	49.4	—	3.91	1.54	—	—	—	97.1
	Aubres	0.39	—	33.0	1.58	8.12	—	0.02	0.11	0.00	50.4	0.00	1.84	1.40	0.00	—	—	96.9
	Cumberland Falls	0.05	—	33.3	1.57	8.86	—	0.00	0.05	1.54	48.1	0.03	3.71	1.89	0.02	—	—	99.1
	Khor Temiki	0.11	—	33.1	1.68	8.21	—	0.02	0.00	0.05	52.8	0.00	1.41	1.99	0.00	—	—	99.3
	Peña Blanca Spring	0.11	—	32.5	1.51	9.10	—	0.46	0.30	0.07	52.9	0.00	0.57	1.65	0.00	—	—	99.2
Mineral-A	Y-793592	0.66	—	42.3	—	0.45	—	—	34.3	0.09	0.60	—	—	—	—	0.21	—	78.5
	Bustee	0.83	—	48.1	—	0.94	0.05	1.21	38.2	0.05	0.05	—	—	—	—	—	—	89.4
Mineral-B	Y-793592	3.22	—	35.4	—	0.81	—	—	26.3	0.03	0.00	—	—	—	—	0.01	—	65.7
	Bustee	1.77	—	41.0	—	1.76	1.39	0.85	34.0	0.05	0.05	—	—	—	—	—	—	80.9
Troilite	Y-793592	—	—	37.2	—	—	—	1.40	0.18	0.07	59.8	—	—	—	0.00	—	—	98.7
	ALH-78113	—	—	37.4	—	—	—	0.85	0.53	0.08	60.8	—	—	—	0.00	—	—	99.7
	Bustee	—	—	36.6	—	—	—	6.91	0.45	0.05	55.6	—	—	—	—	—	—	99.7

—: not analyzed.

*: This alabandite analysis overlaps with new Ag-sulfide reported by LIN et al. (1989).
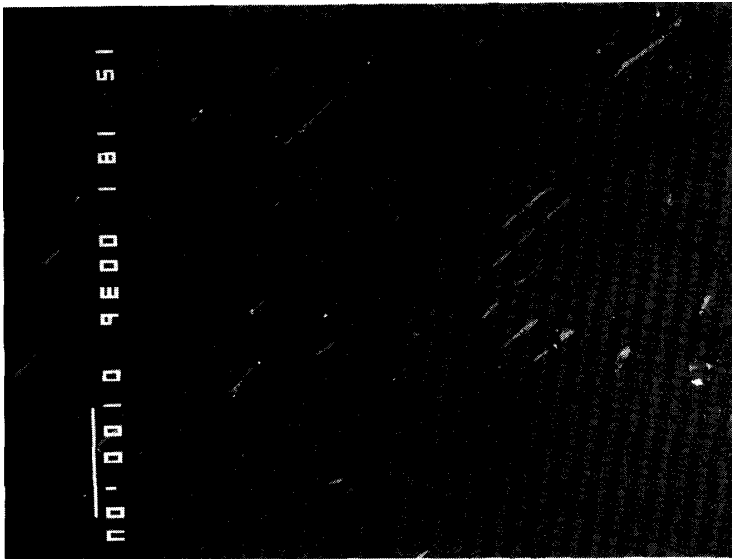
Fig. 2a. Coarse-grained en-
statite fragments with diop-
side lamellae (bright laths)
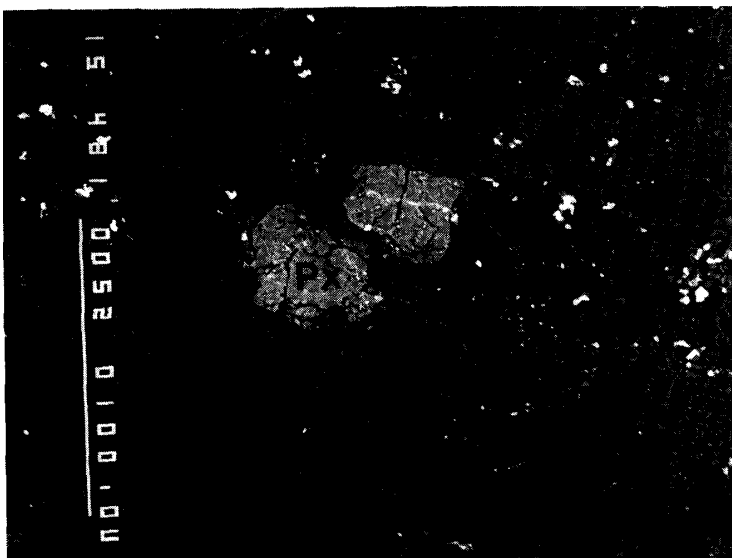in ALH-78113. BSE image.
White scale bar of 100 μm.

Fig. 2b. Isolated FeO-rich
pyroxene fragments (Px) in
the matrix consisting of
enstatite in ALH-78113.
BSE image. White scale bar
of 100 μm.

Fig. 2c. Troilite fragments
(Tr) with thin daubreelite
lamellae (dark laths) in
ALH-78113. BSE image.
White scale bar of 10 μm.

Fig. 2d. Intergrowth of ala-
bandite (Al) and troilite
(Tr) in ALH-78113. Ala-
bandite has thin lamellae
which seem to be troilite.
BSE image. White scale bar
of 10 μm.
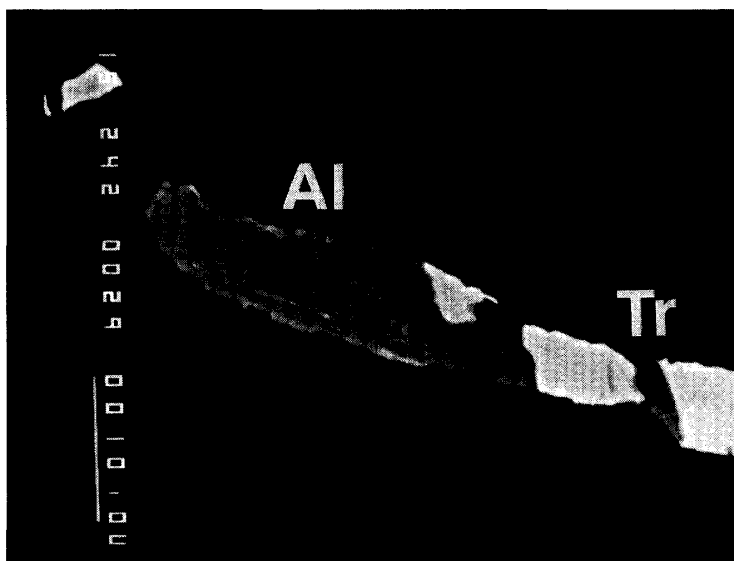
Fig. 2e. Intergrowth of djerfi-
sherite (Dj) and troilite (Tr)
in ALH-78113. Kamacite
(Ka) occurs near this grain.
BSE image. White scale bar
of 10 μm.
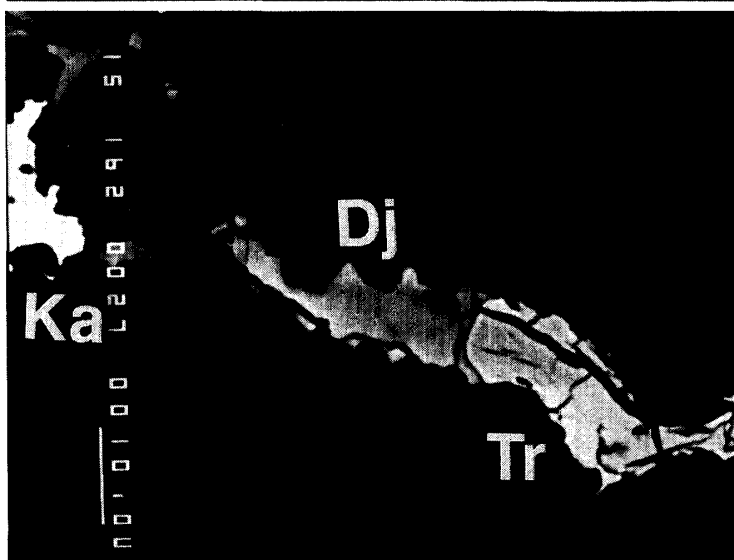
Fig. 2f. A dark clast consist-
ing of enstatite (En) and
FeO-rich Ca-poor pyroxene
(Px) with fine-grained oli-
vine and opaque minerals
(bright) in ALH-78113.
BSE image. White scale bar
of 10 μm.
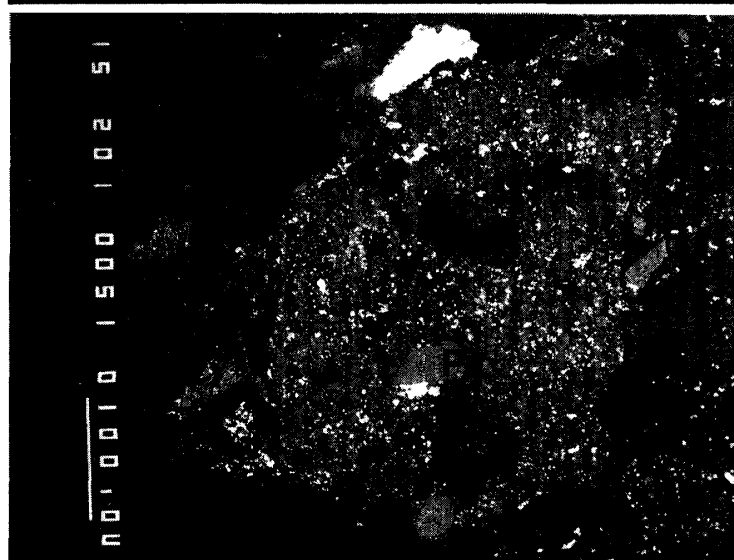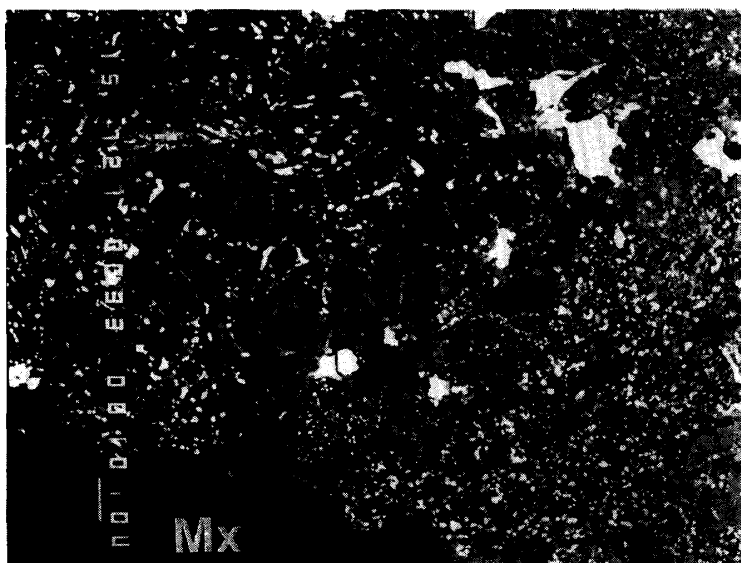
Fig. 2g. Ca-poor pyroxene (Px) and olivine (Ol) in a dark clast in ALH-78113. Note that pyroxenes have euhedral forms and show normal zoning from FeO-poor cores (dark) to FeO-rich rims (gray). The interstices between pyroxenes is filled by plagioclase and glass. Fine-grained opaque minerals such as Fe-Ni metal and troilite (bright) abundantly occur in the dark clast. The boundary between the dark clast and the matrix (Mx) is sharp. BSE image. White scale bar of 10 μm.

have 0.7–1.8 and 1.6–3.2 wt% Na, 0.5–0.6 and 0.4–0.8% K, 39.3–42.3 and 35.5–35.4% S, and 32.3–34.3 and 25.3–26.3% Cr, respectively. Some grains have a small content of Zr (0.2%). Totals of minerals A and B are 63.7–65.7 and 74.4–78.5 wt%, respectively.

3.2. ALH-78113

ALH-78113 is also a breccia consisting mainly of enstatite fragments and fine-grained matrix. Our thin section (ALH-78113,102-1) has no chondritic clasts reported in ALH-78113 (Lipschutz *et al.*, 1988). Instead, ALH-78113 studied here has several dark-colored and irregular-shaped clasts (hereafter dark clasts), 200–300 μm in size (Table 1). ALH-78113 also has suffered shock metamorphism.

Compositional range of enstatite, except that in dark clasts, is $En_{97.8-99.8}$ $Fs_{0.0-0.6}Wo_{0.1-2.2}$ (Table 2). Some coarse-grained enstatites have thin lamellae of diopside up to 10 μm in width (Fig. 2a). Isolated FeO-rich pyroxene fragments rarely occur in the matrix (Fig. 2b). These pyroxenes ($En_{77.8-80.6}Fs_{18.8-21.3}Wo_{0.4-1.0}$) have similar compositions to FeO-rich pyroxenes in the dark clasts as mentioned later. Diopside ($En_{51.5-55.8}Fs_{0.0-0.9}Wo_{44.2-48.0}$) often has lamellae of enstatite. Olivine is pure forsterite. Compositional range of plagioclase ($Ab_{28.4-97.6}An_{0.0-70.6}Or_{0.2-5.2}$) in ALH-78113 is much wider than that of Y-793592 (Fig. 3). Glass is rich in SiO_2 (58.6–85.1 wt%), Al_2O_3 (3.2–21.5%) and Na_2O (1.0–10.3%). A few grains of a silica mineral have Al_2O_3 (1.3–1.9 wt%) and Na_2O (0.6–0.8%).

Opaque minerals occur more abundantly in ALH-78113 than in Y-793592, and most of them occur in the matrix. Kamacite and taenite have 1.5–5.8 and 38.8–51.4 wt% Ni, respectively (Table 3). Schreibersite has 22.1–58.8 wt% Ni. Troilite is abundantly accompanied by daubreelite lamellae, 1–10 μm in width (Fig. 2c). Troilite has 0.4–1.7 wt% Ti and 0.2–0.7% Cr (Table 4). Although the Ti content of troilite in ALH-78113 is lower than that in Y-793592 (Fig. 4), this is within the range (0.5–5.7%) of non-Antarctic aubrites (Watters and Prinz, 1979). Daubreelites have 0.7–1.8 wt% Mn and 0.0–0.3% Zn. Some alabandite grains have thin lamellae, 1–2 μm in width,
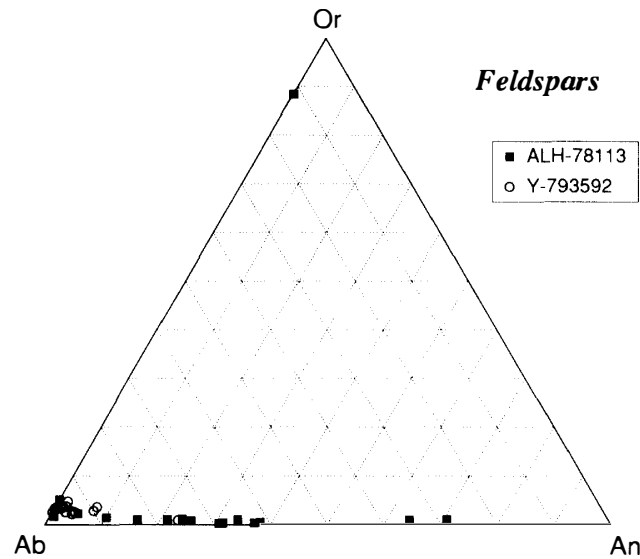
Fig. 3. Molar plot of orthoclase (Or)—albite (Ab)—anorthite (An) of feldspars in Y-793592 and ALH-78113. K-feldspar occurs in a dark clast in ALH-78113. Plagioclases, especially in ALH-78113, have wide compositional variations.
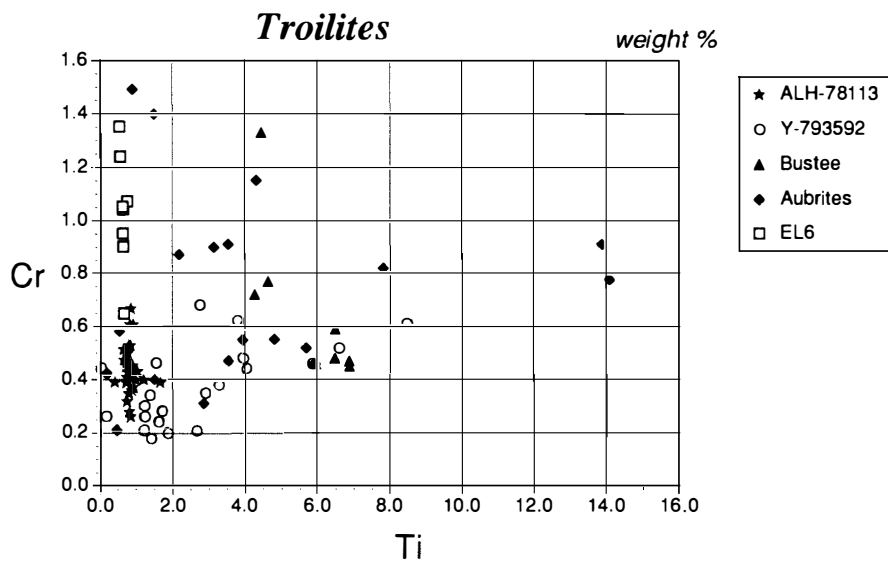

Fig. 4. Ti-Cr (wt%) plot for troilites in aubrites and EL6 chondrites (KEIL, 1968b). Troilites in aubrites are usually enriched in Ti.

which seem to be troilite (Fig. 2d). Alabandite has 47.2–54.3 wt% Mn, 0.3–0.6% Mg and 7.0–14.4% Fe. Djerfisherite occurs often with troilite and alabandite (Fig. 2e), and has 0.1–0.7 wt% Na, 8.1–9.2% K, 3.5–4.4% Ni and 0.9–1.5% Cu. WATTERS et al. (1980) reported oldhamite in ALH-78113, which is not encountered in our thin section.

Dark clasts are aggregates of fine-grained silicate phases, up to 30 μm in size, with abundant opaque minerals (Fig. 2f). Pyroxene is the predominant mineral, but in some dark clasts olivine is also abundant, up to about 50 vol%. The interstices among pyroxene and olivine are filled by glass or feldspar (Fig. 2g). The boundary between the dark

clast and the matrix is often sharp. Ca-poor pyroxenes in the dark clasts have a wide compositional range, $En_{77.5-98.9}Fs_{0.3-20.5}Wo_{0.3-2.9}$ (Table 2). Some euhedral pyroxene grains show a normal zoning (e.g., $Fs_{9.7}$ to $Fs_{15.7}$). On the other hand, FeO-rich pyroxenes have corroded or irregular-shaped outlines without a zoning (Fig. 2f). Diopside ($En_{52.9-59.0}Fs_{0.0-4.2}Wo_{40.6-45.3}$) and olivine ($Fo_{98.7-100.0}$) often have minor FeO contents. The dark clasts usually include sodic to calcic plagioclase ($Ab_{35.0-95.7}$). A dark clast has K-feldspar ($Ab_{11.5}An_{0.1}Or_{88.4}$). This is the first discovery from aubrite. Glass has minor FeO content (0.1–3.8 wt%). Fine-grained opaque minerals in the dark clasts are kamacite, taenite, schreibersite, troilite, alabandite and daubreelite (Table 1), which have compositions similar to those in the matrix.

4. Discussion

4.1. Thermal history of ALH-78113 and Y-793592

Equilibrium temperature for ALH-78113 is estimated to be about 500°C using Co partitioning between coexisting kamacite (0.55–0.68 wt% Co) and taenite (0.17–0.14% Co) after the method by AFIATTALAB and WASSON (1980). Equilibrium temperature between kamacite (1.5–5.1 wt% Ni and <0.05% P) and schreibersite (22.5–58.8% Ni and 15.4% P) in ALH-78113 is 400–500°C, using the phase diagram of Fe-Ni-P by ROMIG and GOLDSTEIN (1980). Alabandite coexisting with troilite in ALH-78113 has too low Fe content to be applied to a geothermometer. These low equilibration temperatures for ALH-78113 are consistent with the occurrences of lamellae of diopside in enstatite, enstatite in diopside, daubreelite in troilite, and troilite in alabandite. Y-793592 has no pair of metallic phases and sulfides to be applied to a geothermometer. However, rare or no occurrence of lamellae in pyroxenes and sulfides in Y-793592 suggests more rapid cooling than ALH-78113.

Both aubrites experienced later shock metamorphism as mentioned in Section 3.1. Some other aubrites as well as Y-793592 and ALH-78113, have interstitial glass (FUCHS, 1974; OKADA et al., 1988). Such a glass, enriched in normative feldspar, occurs in the brecciated matrix. It is possible that the partial melting took place by shock-induced heating.

4.2. Dark clasts in ALH-78113

NEAL and LIPSCHUTZ (1981), and LIPSCHUTZ et al. (1988) reported fine-grained chondritic inclusions, larger than several mm across, in Cumberland Falls and ALH-78113. They consist mainly of olivine (Fo_{79-99} and 10–51 vol%), low-Ca pyroxene (En_{74-99} and 17–56 vol%) with diopside, glass and various accessory minerals. These inclusions represent an unknown chondrite suite, and they originated under a broad redox range (LIPSCHUTZ et al., 1988). The mineral assemblage, abundance and composition in the dark clasts reported here resemble those of such chondritic inclusions. A few dark clasts have abundant olivine like some chondritic inclusions. FeO-rich pyroxene occurs in the dark clasts, whose composition is within the range of the chondritic inclusions. Therefore, the chondritic inclusions and the dark clasts may have a cogenetic origin; they were probably derived from a common precursor, although the dark clasts represent a small sized fraction. Isolated FeO-rich pyroxenes in the matrix

of ALH-78113 are also fragments derived by disaggregation of such materials.

The euhedral forms of olivine and pyroxene with normal zoning, and the interstitial glass in the dark clasts suggest that these dark clasts were once melted. On the other hand, FeO-rich pyroxenes with corroded outline in the dark clasts may be relics from the precursor. The dark clasts occur in fine-grained and brecciated matrix, suggesting that the dark clasts experienced melting probably by shock-induced heating.

4.3. Comparison of mineralogy of aubrite and enstatite chondrites
4.3.1 Roedderite

Roedderite occurs in Qingzhen, Y-691, ALH-77295 (EH3), Y-74370, Indarch (EH4) and Abee (EH5) (KIMURA and EL GORESY, 1988). The $Na/Na+K$ ratio of roedderite increases in the order of EH3 (0.52–0.59), EH4 (0.63–0.68) and EH5 (0.78) (Fig. 5). Roedderite in Y-793592 is enriched in K_2O (atomic $Na/Na+K$ ratio 0.49–0.54) like those in EH3. The bulk $Na/Na+K$ atomic ratio of Y-793592 is 0.93 after YANAI (1992), and the K_2O-rich roedderite seems to be complementary to sodic plagioclase ($Na/Na+K$ ratio 0.97 on average) in Y-793592, although glass (0.90), and rare Na-Cr-sulfide (0.82) and djerfisherite (0.06) also contain K_2O. The FeO contents of Y-793592 roedderite is the lowest among enstatite meteorites (Fig. 5), suggesting that it formed under the most reducing condition.

Roedderite coexists with albitic plagioclase (mostly $An_3 >$) in EH chondrites and Y-793592. Distribution coefficients of $Na/Na+K$ ratios between roedderite and albite, $(X/1-X)_{Roedderite}/(X/1-X)_{Albite}$ where X is mole fraction of Na, seem to reversely correlate with petrologic type (Fig. 6); the coefficients are 0.142 for EH5, 0.021–0.072 for EH4 and 0.003–0.009 for EH3. Such a correlation may reflect a formation temperature of roedderite and albite in these meteorites. SKINNER and LUCE (1971) concluded that
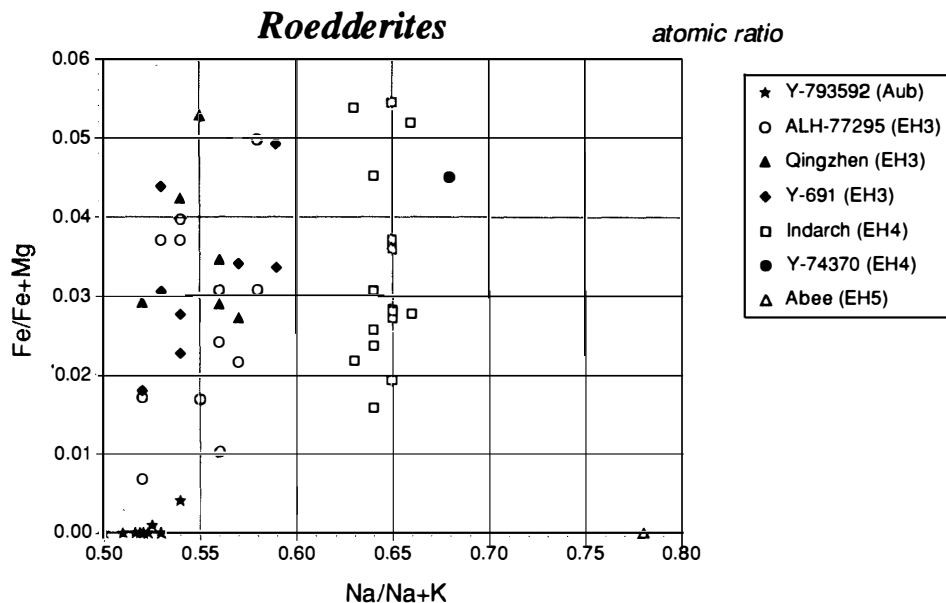

Fig. 5. $Na/Na+K$ vs. $Fe/Fe+Mg$ (atomic ratio) plot for roedderites in Y-793592 and EH3-5 chondrites (KIMURA and EL GORESY, 1988). Roedderites in Y-793592 is enriched in Na like those in EH3, but they are almost free of FeO.
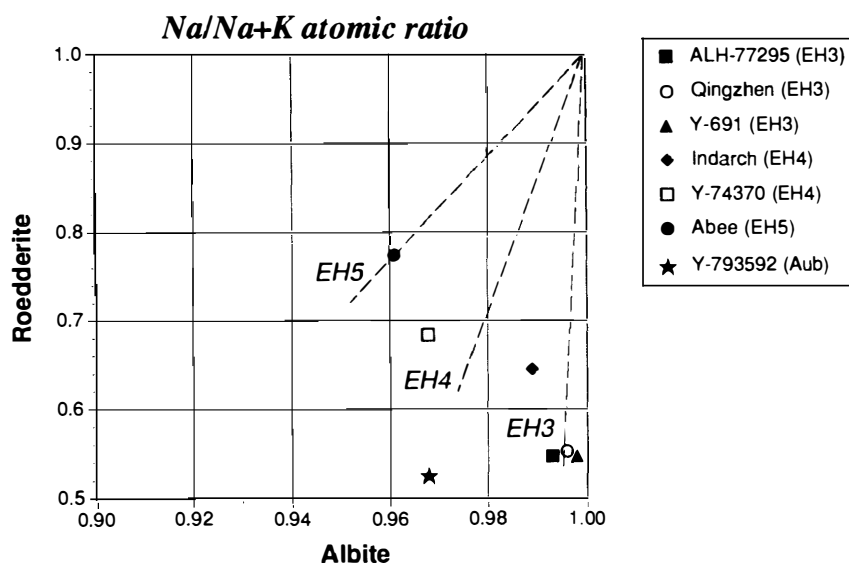
Fig. 6. Rooseboom diagram of Na/Na+ K atomic ratios for coexisting roedderite and albite in Y-793592 and EH3–5 chondrites after KIMURA and EL GORESY (1988).

temperatures for niningerite formation in Abee (EH5) and Indarch (EH4) were 700–800°C and 500–600°C, respectively. However, the other EH3-4 chondrites in Fig. 6 have too low-Fe niningerite (EHLERS and EL GORESY, 1988) to be applied to the geothermometer by SKINNER and LUCE (1971). However, pairs of roedderite and albite in petrologic type 3 may have formed at a temperature lower that those in higher types. The coefficient for Y-793592 is 0.036 which is within the range of EH4, suggesting that a formation temperature of roedderite-albite pair in Y-793592 is lower than that in EH5 and higher than EH3. Such a low temperature for Y-793592 may reflect the final cooling stage, where equilibration took place between the metallic phases.

4.3.2. Daubreelite

Daubreelites in Y-793592 and ALH-78113 have low Zn content (<0.3%) (Fig. 7). Daubreelites in non-Antarctic aubrites are also poor in Zn (WATTERS and PRINZ, 1979; this study). On the other hand, daubreelites in EH chondrites are enriched in Zn (0.7–8.1%) (KEIL, 1968a; EL GORESY et al., 1988; LIN, 1991; KIMURA, unpublished data), except for South Oman (E4) having Zn-poor daubreelite (0.0–0.3 wt%). However, South Oman is an unusual enstatite chondrite, which has K-feldspar instead of K-bearing sulfide (KIMURA and EL GORESY, 1988). Such an anomalous nature of South Oman is also reflected in the unusual rare gas compositions (CRABB and ANDERS, 1981). Daubreelites in EL6 chondrites are also depleted in Zn (KEIL, 1968b), like those in aubrites.

Zinc contents of daubreelites in aubrite and EL6 are evidently lower than those in EH3–5 (Fig. 8). Aubrite and EL6 are also poor in bulk Zn content. Zinc prefers sphalerite to the other minerals in enstatite meteorites. However, sphalerite is not encountered in aubrites, and Zn is detected only in daubreelites in aubrites studied here. Therefore, the low-Zn contents of daubreelites in aubrites reflect low bulk Zn contents in aubrites. WOLF et al. (1983) reported the depletion of volatile elements such as Zn and In in aubrite, and suggested that a parent body of aubrite is depleted in volatile elements.
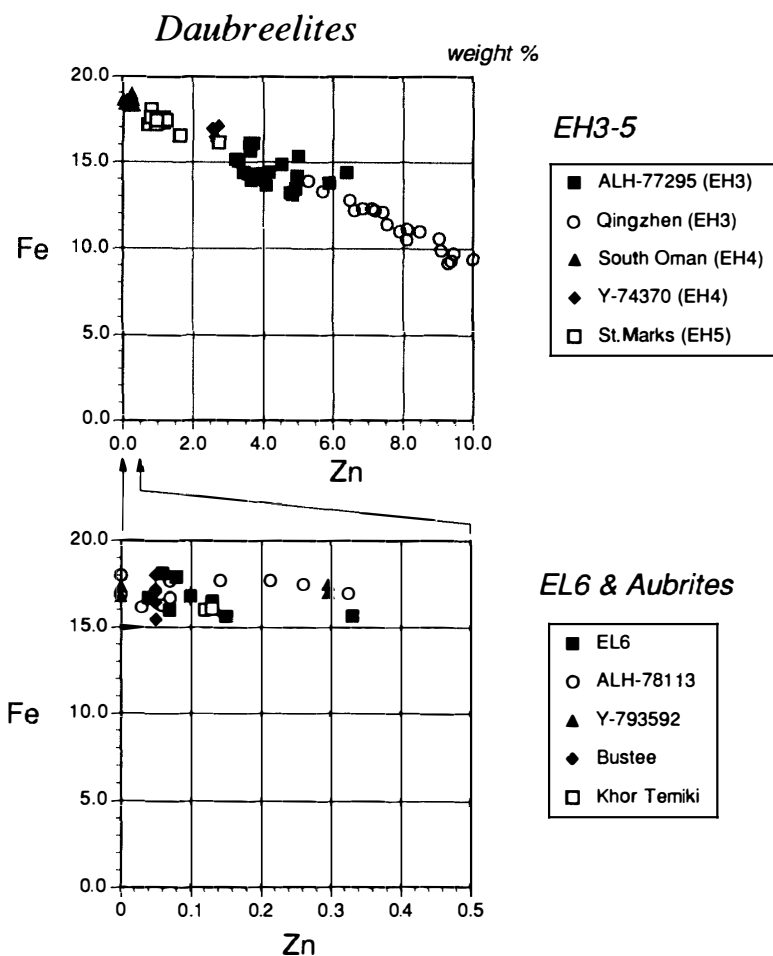
Fig. 7. Zn-Fe (wt%) plot for daubreelites in aubrites, EL6 (KEIL, 1968b) and EH3-5 chondrites (LIN, 1991; KIMURA, unpublished data). Note that daubreelites in aubrites and EL6 chondrites are extremely poor in Zn, in comparison with those in EH chondrites.

4.3.3. Djerfisherite

We found djerfisherite in Y-793592, ALH-78113, Aubres, Cumberland Falls, Khor Temiki and Peña Blanca Spring. In addition, EL GORESY et al. (1971) reported djerfisherite from the Bishopville aubrite. Thus, djerfisherite is a common accessory mineral in aubrites. Djerfisherites in aubrites are characterized by low contents of Cu (0.9–2.3 wt%) and Na ($<0.7\%$), and high content of Ni (0.4–5.5%) (Table 4). On the other hand, djerfisherites in EH3 chondrites are enriched in Cu (1.3–5.0 wt%) and Na (0.4–1.9%), whereas poor in Ni (0.4–3.1%) (KIMURA and EL GORESY, 1988; LIN, 1991). Those in EH4-5 are poor in Na (<0.2 wt%), but rich in Cu (2.4–7.4%) (Fig. 9). Thus, djerfisherite in aubrite is distinguished from those in EH3-5 by its chemical composition.

FUCHS (1966) assigned the chemical formula $K_3(Na, Cu)(Fe, Ni)_{12}S_{14}$ to a djerfisherite from Indarch (EH4). Later CZAMANSKE et al. (1979) determined the crystal structure of a terrestrial djerfisherite and the formula as $K_6Na_1(Fe, Cu, Ni)_{24}S_{26}Cl_1$. Average chemical formulae of meteoritic djerfisherites are $(K, Na)_6(Fe, Cu, Ni, Co)_{24}S_{26}Cl_1$ in aubrites and $(K, Na)_6(Fe, Cu, Ni, Co)_{25}S_{26}Cl_1$ in EH chondrites.
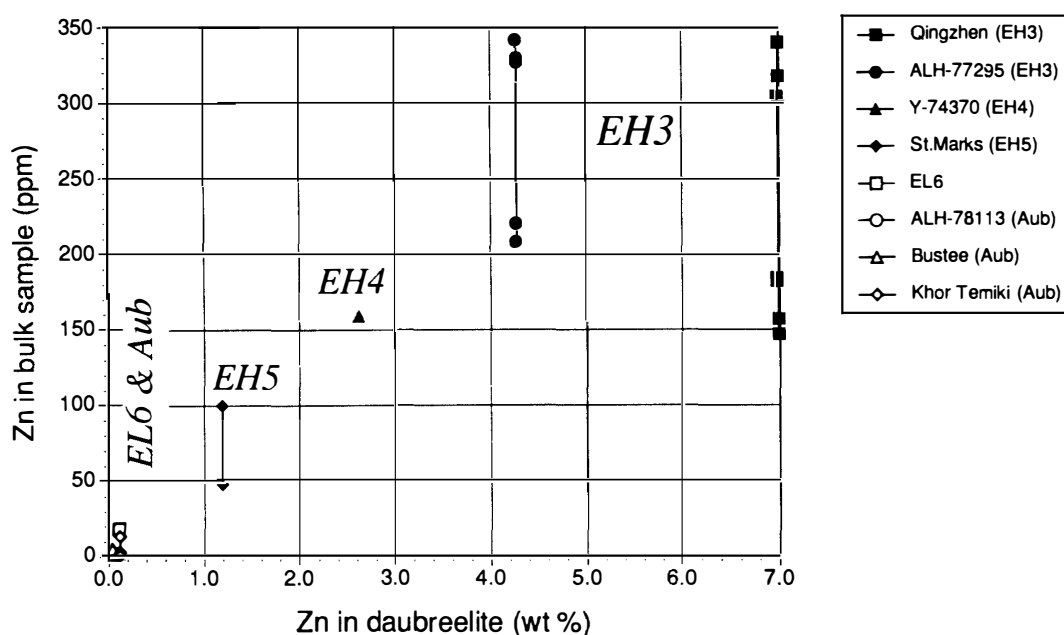
Fig. 8. Plot of average Zn in daubreelite (wt%) vs. Zn in bulk sample (ppm). Bulk data are quoted
         as follows: Qingzhen after Weeks and Sears (1985), Kallemeyn and Wasson (1986),
         El Goresy et al. (1988), and Kaczaral et al. (1988), ALH-77295 after Kallemeyn and
         Wasson (1986), and Weeks and Sears (1985), Y-74370, St. Marks and average EL6
         after Kallemeyn and Wasson (1986), ALH-78113 after Biswas et al. (1980), and Bustee
         and Khor Temiki after Biswas et al. (1980) and Wolf et al. (1983).

4.3.4. Na-Cr-sulfide

Minerals A and B occur in Bustee as well as Y-793592, although the total is higher in Bustee (Table 4), probably due to small grain size of Na-Cr-sulfides in Y-793592. From semi-quantitative analyses, minerals A and B in ALH-77295 (EH3), Qingzhen (EH3) and Bustee have about 6–7 and 11–15 wt% oxygen, probably as H_2O or OH. Thus, these minerals may have formed by aqueous alteration, probably during terrestrial weathering. High content of oxygen in mineral B is consistent with lower total weight percents (71–79 wt%) than mineral A (88–93%).

Minerals A and B were also reported from Peña Blanca Spring, Norton County and Pesjanoe aubrites (Ramdohr, 1973). The other two Na-Cr-sulfides, caswellsilverite and schöllhornite, have been reported in Norton County (Okada and Keil, 1982; Okada et al., 1985). Atomic Cr/S ratios of caswellsilverite, schöllhornite, and minerals A and B are nearly 1/2. However, alkali is depleted in schöllhornite ($Na_{0.3}CrS_2$), and especially in minerals A ($[Na, K]_{0.07}Cr_{0.99}S_2$ on average) and B ($[Na, K]_{0.12}Cr_{1.00}S_2$), in comparison to caswellsilverite ($NaCrS_2$). K is always contained in minerals A and B in Y-793592 and Bustee (Na/Na + K ratio 0.18–0.87), whereas schöllhornite has no detectable K. Thus, minerals A and B may be different phases from schöllhornite (El Goresy et al., 1988). At any rate, Na-Cr-sulfide had primarily occurred in many aubrites.

4.4. Genetic relationships between aubrite and enstatite chondrites

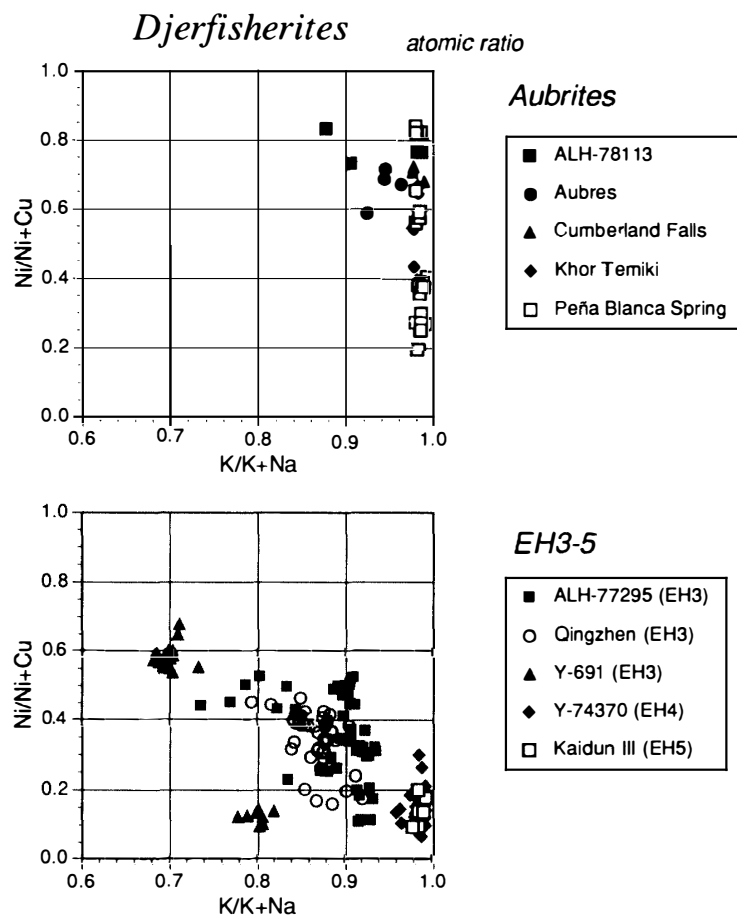Djerfisherite, Na-Cr-sulfide and roedderite are also found in almost all EH3–5

Fig. 9. $Ni/Ni + Cu$ vs. $K/K + Na$ atomic ratio plot for djerfisherites in aubrites and EH3–5 chondrites. Djerfisherites in aubrites can be distinguished by low-Na and high-Ni contents from those in EH chondrites.

chondrites (Table 1). However, aubrites have no niningerite and sphalerite that are common accessory minerals in EH3–5. In addition, the compositions of daubreelite, djerfisherite and roedderite in aubrites are evidently different from those in EH3–5. Thus, these minerals were not xenocrystic fragments from EH chondrite.

Djerfisherite, Na-Cr-sulfide, roedderite and caswellsilverite have not been reported in EL chondrites, except for djerfisherite in MAC88136, EL3 (LIN et al., 1991) and mineral A in Khaipur, EL6 (RAMDOHR, 1973). Alkali elements may have formed only feldspar in EL6 chondrites. Thus, the mineral assemblages of aubrite and EL are not the same. IKEDA (1989) proposed that these alkali-bearing minerals in EH3 were formed by fractionation of Al_2O_3 relative to alkali elements during condensation in the nebula. From this model, these minerals may be expected to be not encountered in EL6 which have high $Al/Al + Na + K$ ratio (0.59 on average) after KALLEMEYN and WASSON (1986). On the other hand, aubrites have lower ratio (0.46 on average) after NTAFLOS and KOEBERL (1992). The precursor material of aubrites may also have suffered the fractionation of Al_2O_3 in the nebula like EH chondrites, or in a parent body by a magmatic process. Excess alkali elements relative to Al_2O_3 should have formed djerfisherite, Na-Cr-sulfide and roedderite in aubrites. The different mineral assemblage

in aubrites observed here, may reflect a precursor material different from EL6, being consistent with BRETT and KEIL (1986) and KEIL (1989).

Acknowledgments

References

AFIATTALAB, F. and WASSON, J. T. (1980): Composition of the metal phases in ordinary chondrites: Implications regarding classification and metamorphism. Geochim. Cosmochim. Acta, **44**, 431–446.

BISWAS, S., WALSH, T., BART, G. and LIPSCHUTZ, M. E. (1980): Thermal metamorphsim of primitive meteorites—XI. The enstatite meteorites: origin and evolution of a parent body. Geochim. Cosmochim. Acta, **44**, 2097–2110.

BRETT, R. and KEIL, K. (1986): Enstatite chondrites and enstatite achondrites (aubrites) were not derived from the same parent body. Earth Planet. Sci. Lett., **81**, 1–6.

CRABB, J. and ANDERS, E. (1981): Noble gases in E-chondrites. Geochim. Cosmochim. Acta, **45**, 2443–2464.

CZAMANSKE, G. K., ERD, R. C., SOKOLOVA, M. N., DOBROVOL'SKAYA, M. G. and DMITRIEVA, M. T. (1979): New data on rasvumite and djerfisherite. Am. Mineral., **64**, 776–778.

EHLERS, K. and EL GORESY, A. (1988): Normal and reverse zoning in niningerite: A novel key parameter to the thermal histories of EH-chondrites. Geochim. Cosmochim. Acta, **52**, 877–887.

EL GORESY, A., GRÖGLER, N. and OTTEMANN, J. (1971): Djerfisherite composition in Bishopville, Pena Blanca Springs, St. Marks and Toluca meteorites. Chem. Erde, **30**, 77–82.

EL GORESY, A., YABUKI, H., EHLERS, K., WOOLUM, D. and PERNICKA, E. (1988): Qingzhen and Yamato-691: A tentative alphabet for the EH chondrites. Proc. NIPR Symp. Antarct. Meteorites, **1**, 65–101.

FUCHS, L. H. (1966): Djerfisherite, alkali-copper-iron sulfide: A new mineral from enstatite chondrites. Science, **153**, 166–167.

FUCHS, L. H. (1974): Glass inclusions of granitic compositions in orthopyroxenes from three enstatite achondrites. Meteoritics, **9**, 342.

IKEDA, Y. (1989): Petrochemical study of the Yamato-691 enstatite chondrite (E3) IV: Descriptions and mineral chemistry of opaque-mineral nodules. Proc. NIPR Symp. Antarct. Meteorites, **2**, 109–146.

KACZARAL, P. W., DENNISON, J. E., VERKOUTEREN, R. M. and LIPSCHUTZ, M. E. (1988): On volatile/mobile trace element trends in E3 chondrites. Proc. NIPR Symp. Antarct. Meteorites, **1**, 113–121.

KALLEMEYN, G. W. and WASSON, J. T. (1986): Compositions of enstatite (EH3, EH4, 5 and EL6) chondrites: Implications regarding their formation. Geochim. Cosmochim. Acta, **50**, 2153–2164.

KEIL, K. (1968a): Zincian daubreelite from the Kota-Kota and St. Marks enstatite chondrites. Am. Mineral., **53**, 491–494.

KEIL, K. (1968b): Mineralogical and chemical relationships among enstatite chondrites. J. Geophys. Res., **73**, 6945–6976.

KEIL, K. (1969): Titanium distribution in enstatite chondrites and achondrites, and its bearing on their origin. Earth Planet. Sci. Lett., **7**, 243–248.

KEIL, K. (1989): Enstatite meteorites and their parent bodies. Meteoritics, **24**, 195–208.

KIMURA, M. and EL GORESY, A. (1988): Djerfisherite compositions in EH chondrites: A potentital parameter to the geochemistry of the alkali elements. Meteoritics, **23**, 279–280.

LIN, Y.-T. (1991): Qingzhen enstatite chondrite (EH3): petrology, mineral chemistry and evolution. Ph. D. Thesis, Institute of Geochemistry, Guanzhou, China, 135 p. (in Chinese).

LIN, Y.-T., EL GORESY, A. and HUTCHEON, I. D. (1989): The first meteoritic siliver minerals in Peña Blanca Springs enstatite achondrtie: Assemblages, compositions and silver isotopes. Lunar and Planetary Science XX. Houston, Lunar Planet. Inst., 572–573.

LIN, Y.-T., NAGEL, H.-J., LUNDBERG, L. L. and EL GORESY, A. (1991): MAC88136—The first EL3 chondrite. Lunar and Planetary Science XXII. Houston, Lunar Planet. Inst., 811–812.

LIPSCHUTZ, M. E., VERKOUTERN, R. M., SEARS, D. W. G., HASAN, F. A., PRINZ, M., WEISBERG, M. K., NEHRU, C. E., DELANEY, J. S., GROSSMAN, L. and BOILY, M. (1988): Cumberland Falls chondritic inclusion: III. Consortium study of relationship to inclusions in Allan Hills 78113 aubrite. Geochim. Cosmochim. Acta, 52, 1835–1848.

MAYEDA, T.K. and CLAYTON, R. N. (1980): Oxygen isotopic compositions of aubrites and some unique meteorites. Proc. Lunar Planet. Sci. Conf., 11th, 1145–1151.

NEAL, C. W. and LIPSCHUTZ, M. E. (1981): Cumberland Falls chondritic inclusions: Mineralogy/petrology of a forsterite chondite suite. Geochim. Cosmocim. Acta, 45, 2091–2107.

NTAFLOS, Th. and KOEBERL, C. (1992): Petrological studies and bulk chemical analyses of eight antarctic aubrites. Lunar and Planetary Science XXIII. Houston, Lunar Planet. Inst., 1003–1004.

OKADA, A. and KEIL, K. (1982): Caswellsilverite, $NaCrS_2$: a new mineral in the Norton County enstatite achondrite. Am. Mineral., 67, 132-136.

OKADA, A., KEIL, K., LEONARD, B. F. and HUTCHEON, I. D. (1985): Schöllhornite, $Na_{0.3}(H_2O)_1[CrS_2]$, a new mineral in the Norton County enstatite achondrite. Am. Mineral., 70, 638–643.

OKADA, A., KEIL, K., TAYLOR, G. J. and NEWSOM, H. (1988): Igneous history of the aubrite parent asteroid: Evidence from the Norton County enstatite achondrite. Meteoritics, 23, 59–74.

RAMDOHR, P. (1973): The Opaque Minerals in Stony Meteorites. Amsterdam, Elsevier, 245 p.

ROMIG, A. D. and GOLDSTEIN, J. I. (1980): Determination of the Fe-Ni and Fe-Ni-P phase diagrams at low temperatures (700 to 300°C). Metall. Trans., 11A, 1151–1159.

SKINNER, B. J. and LUCE, F. D. (1971): Solid solutions of the type (Ca, Mg, Mn, Fe)S and their use as geothermometers for the enstatite chondrites. Am. Mineral., 56, 1269–1296.

WATTERS, T. R. and PRINZ, M. (1979): Aubrites: Their origin and relationship to enstatite chondrites. Proc. Lunar Planet. Sci. Conf., 10th, 1073–1093.

WATTERS, T. R., PRINZ, M., RAMBALDI, E. R. and WASSON, J. T. (1980): ALHA 78113, Mt. Egerton and the aubrite parent body. Meteoritics, 15, 386.

WEEKS, K. S. and SEARS, D. W. G. (1985): Chemical and physical studies of type 3 chondrites-V: The enstatite chondrites. Geochim. Cosmochim. Acta, 49, 1525–1536.

WOLF, R., EBIHARA, M., RICHTER, G. R. and ANDERS, E. (1983): Aubrites and diogenites: Trace elements clues to their origin. Geochim. Cosmochim. Acta, 47, 2257–2270.

YANAI, K. (1992): Yamato-793592: The first enstatite achondrite (aubrite) in the Yamato meteorite collections. Proc. NIPR Symp. Antarct. Meteorites, 5, 235–241.

YANAI, K. and KOJIMA, H. (1991): Yamato-793592: The first enstatite achondrite (aubrite) in the Yamato meteorite. Papers Presented to the 16th Symposium on Antarctic Meteorites, June 5–7, 1991. Tokyo, Natl Inst. Polar Res., 5–7.